Zygote **15** (August), pp. 273–283. © 2007 Cambridge University Press
doi:10.1017/S0967199407004297 Printed in the United Kingdom

Ultrastructural changes in the follicular epithelium of *Ceratophrys cranwelli* previtellogenic oocytes

E.I. Villecco, M.E. Mónaco and S.S. Sánchez

Departamento de Biología del Desarrollo, Instituto Superior de Investigaciones Biológicas (INSIBIO), Consejo Nacional de Investigaciones Científicas y Técnicas (CONICET) y Universidad Nacional de Tucumán (UNT), Chacabuco 461, 4000, San Miguel de Tucumán, Tucumán, Argentina

Date submitted: 04.12.06. Date accepted: 29.01.07

Summary

In this work we carried out ultrastructural, autoradiographic and biochemical analyses of the follicular epithelium during *C. cranwelli* previtellogenesis. This study revealed that the follicular epithelium in early previtellogenesis is constituted of a single layer of squamous homogeneous cells. During mid-previtellogenesis two types of cells develop: dark cells and clear cells. The follicular dark cells are actively involved in the synthesis of RNA, which is transferred to the oocyte through the interface. In late previtellogenesis the dark cells show apoptotic characteristics such as chromatin condensation, DNA fragmentation and cytoplasm shrinkage. This process forms apoptotic bodies that seem to be engulfed by the oocyte. Our results show evidence that, during mid- and late *C. cranwelli* previtellogenesis, the follicular epithelium undergoes remodelling processes interacting with the oocyte.

Keywords: Amphibian, Apoptosis, Follicular cells, Previtellogenic oocyte

Introduction

In all vertebrates, oogenesis is a complex process characterized by a series of cellular and molecular events that take place in the nucleus and cytoplasm of the developing oocytes (Monroy *et al.*, 1983; Sanchez & Villecco 2003). In the ovary, the oocyte and the somatic tissue (follicle cells and theca) form a morphological entity called the ovarian follicle that undergoes structural and functional differentiation (Bachvarova *et al.*, 1992).

Extensive evidence, both direct and indirect, demonstrates that somatic follicle cells execute multiple and variable functions throughout life and at different stages of gamete and follicle development. Follicle cells have been implicated in a number of gonadotrophin-regulated processes involved in oocyte growth and maturation. These include steroidogenesis (Redshaw, 1972; Fortune, 1983; Sretarugsa & Wallace, 1997; Hernandez *et al.*, 2003; Schoenfelder *et al.*, 2003), initiation of yolk protein (vitellogenin) uptake (Dumont, 1978), meiotic arrest (Villecco *et al.*, 1996) and other processes such as vitelline envelope formation (Dumont and Brummett, 1978; Cabada *et al.*, 1996), RNA transfer (Sanchez Riera *et al.*, 1988; Motta *et al.*, 1995) and organelle transfer (Andreuccetti, 1992; Motta *et al.*, 1995).

In many vertebrates, during the different stages of oogenesis, the follicular is arranged as a single layer of homogeneous cells (Callebaut & Van Nassauw, 1987). In contrast, the follicular epithelium of previtellogenic oocytes from lizards and snakes is typically polymorphic and multilayered, being characterized by the presence of three distinct cells: small, intermediate and pyriform cells (Filosa, 1973; Andreuccetti *et al.*, 1979). The heterogeneity of the granulosa cell population disappears from the vitellogenic oocytes by regression of intermediate and pyriform cells via programmed cell death (Motta *et al.*, 1996, 2001).

In both anuran and urodele amphibians studied up to now, the follicles cells form a monolayer of homogeneous structure around each developing oocyte that remains unchanged throughout oocyte growth (Kemp, 1956, Wartenberg, 1960; Hope, 1963, Dumont, 1972; Villecco *et al.*, 1998, 2000).

All correspondence to: S.S. Sánchez, Departamento de Biología del Desarrollo, INSIBIO (CONICET-UNT), Chacabuco 461, 4000-San Miguel de Tucumán, Argentina. Tel: +54 81 4107214. Fax: +54 81 4247752 ext. 7004. e-mail: ssanchez@fbqf.unt.edu.ar

In the present work we investigate the follicular epithelium of *Ceratophrys cranwelli* oocytes, the Argentine horned frog. This species was selected because it is capable of effecting rapid oogenesis when it is stimulated by strong transitory rainfall, a factor that seems to be responsible for the activation of the reproductive process (Tinsley *et al.*, 1996). Moreover, *C. cranwelli* has a pattern of early morphogenesis significantly different from that of the best-studied amphibian, *Xenopus laevis* (Purcell & Keller, 1993).

Materials and methods

Animals

Ceratophrys cranwelli ovarian follicles from specimens recently collected in the neighborhood of Tucumán (Argentina) during the spring–summer period were used in this study.

Tissue preparation for microscopy

Sexually mature females were anesthetized. After laparoscopy, pieces of ovary were carefully dissected to obtain isolated oocytes at different stages (Villecco, 1998), wrapped in their follicle. Isolated follicles were measured with an eyepiece micrometer in a stereoscopic microscope.

Transmission electron microscopy

For thin sectioning, previtellogenic whole follicles were fixed for 4 h at 4 °C in 25% glutaraldehyde in 0.1% M sodium phosphate (pH 7.4). Follicles were washed twice in phosphate buffer and postfixed in 1% osmium tetroxide in the same buffer at 4 °C overnight. Samples were dehydrated in an ethanol series and embedded in Spurr resin. Sections were prepared with a Potter Blum MTI ultramicrotome, stained with lead citrate and uranyl acetate and examined with a Zeiss EM109 electron microscope.

Radioactive labelling

Pieces of ovary from six animals, containing 10 to 15 previtellogenic follicles each, were incubated in Ringer's solution with antibiotics (25 µm/ml penicillin and 50 µm/ml streptomycin) containing 100 µCi/ml of [^{3}H]-adenosine (specific activity 36.7 Ci/mM; New England Nuclear) in a total volume of 500 µl. The follicles were incubated for 5 h in a moist chamber at 20–25 °C.

For pulse–chase experiments, the follicles were rinsed after 5 h and transferred to 1 mM adenosine solution. The chase periods were 4 h, 9 h and 24 h.

After incubation, follicles were fixed in Ancel & Vintemberger solution (Ancel & Vintemberger, 1948), dehydrated and embedded in paraffin–celloidin, according to Manes and Nieto (1983). Serial sections, 4–6 µm thick, were attached to slides.

Autoradiography

Autoradiography was carried out with Ilford K2 liquid emulsion diluted 1:1 with distilled water. Exposure was carried out for 15 days at 4 °C. Exposed slides were developed with a Kodak D19 developer, washed and fixed with sodium thiosulfate. Dried slides were stained with hematoxylin–eosin and mounted for light microscopic observation. Blanks of non-radioactive slides were also run.

Ultrastructural localization of RNA

Tissue preparation

Previtellogenic follicles oocytes were fixed by immersion in 0.1 M phosphate-buffered 1% glutaraldehyde solution for 2 h at room temperature. After fixation, the follicles were washed in the phosphate buffer, dehydrated in graded ethanol and embedded in L.R. White resin according to the usual procedure. Thin sections were mounted on nickel grids and processed by cytochemical labelling.

Preparation of the RNase–gold complexes

The colloidal gold suspension was prepared according to the method of Frens (1973). Four millilitres of 1% aqueous solution of sodium citrate were added to a boiling aqueous solution of 100 ml of 0.01% tetrachloroauric acid and allowed to boil for 5 min. By this procedure, we obtained a monodispersed colloidal sol, which was composed of gold particles with an average size of 144 Å in diameter as determined by TEM. It was adjusted to pH 8.5 with 0.2 M K_2CO_3.

To determine the minimal amount of enzyme necessary for full stabilization of the colloidal gold, a constant volume of colloidal gold (5 ml) was mixed with 0.1 ml of serial dilutions of RNase. After 5 min 0.5 ml of 10% NaCl solution was added and flocculation was judged visually. When flocculation occurs, the red colour of the enzyme–gold complex turns into violet. The minimal amount was found to be 0.005 mg/ml.

For the preparation of the RNase–gold complex, 0.1 to 0.5 mg of RNase dissolved in 0.1 ml H_2O was placed in a siliconized tube and 10 ml of the gold suspension (pH 8.5) was added. The mixtures were centrifuged at 25 000 rpm for 30 min at 4 °C. The RNase–gold complex, a dark red sediment, was carefully recovered and resuspended in 3 ml of phosphate-buffered saline (PBS) containing 0.2 mg/ml polyethylene glycol. The pH of the PBS solution was 7.5.

https://doi.org/10.1017/S0967199407004297 Published online by Cambridge University Press

Cytochemical labelling

For cytochemical labelling the grids were first floated, with the tissue sections on the under-surface, for 5 min on a large drop of PBS. In a second step, the sections were incubated on a drop of one of the RNase–gold complexes. This incubation was carried out for various lengths of time from 5 min to over 2 h at 4 °C, at room temperature and at 37 °C. The grids were then thoroughly washed with PBS and rinsed in distilled water. During the entire procedure care was taken to prevent drying of the sections. They were subsequently stained with uranyl acetate and lead citrate and examined with TEM.

In order to determine the specificity of the labelling, the following control was tested. Tissue sections were incubated with the enzyme–gold complex to which the corresponding substrate (RNA 1 mg/ml) was added (Fig. 4*B*) (see later).

TUNEL assay

In situ TUNEL analyses were performed with ovarian fragments using a commercial assay kit (Apoptosis Detection System, Fluorescein, Promega). Serial section of ovary, 4–6 μm thick, were attached to glass microscope slides. The sections were deparaffined, rehydrated, washed with a hypotonic solution (0.85% sodium chloride) and air dried. Slides were fixed in 4% formaldehyde solution in PBS, pH 7.4. The samples were washed by immersing the slides in PBS for 5 min at room temperature and then washed twice with PBS. Sections were permeabilized with proteinase k (20 μg/ml) for 20 min at room temperature, washed twice with PBS and incubated with TUNEL reagents according to manufacturer's protocols. Two slides each were used for negative and positive controls before incubation with TUNEL. Negative-control slides were incubated as describe above, but without the addition of TdT. Positive-control slides were preincubated in the presence of DNase I for 15 min at 37 °C (100 ng/ml) and then washed twice in PBS before incubation.

After the TUNEL reactions were complete, the slides were washed in PBS, sealed under coverslip with nail polish and examined using an Ilford HP5 (ASA 400) fluorescence microscope equipped with a standard filter set for visualization of green fluorescence of fluorescein isothiocyanate-12-dUTP-labelled-DNA (fragmented DNA) within the apoptotic follicle cells.

Results

Follicular epithelium of early previtellogenic oocytes

The ultrastructural analyses of early previtellogenic follicles show a follicular epithelium made up of a single layer of squamous cells forming a continuous monolayer that surrounds the oocyte. Adjacent cells exhibit superposition among them on the marginal zone. The plasma membrane of the follicular cells is in close apposition to the oocyte membrane and they have a clear cytoplasm (Fig. 1*A*, *B*).

In superficial follicular sections, follicle cells show a polygonal shape, with a large round nucleus and electron-lucent cytoplasm (clear cells). The nucleus has a prominent nucleolus and highly dispersed chromatin and is surrounded by a thin layer of cytoplasm with few ribosomes and cisternae of rough endoplasmic reticulum and mitochondria (Fig. 1*C*).

Follicular epithelium of mid-previtellogenic oocytes

The ultrastructural analyses of the follicular epithelium of mid-previtellogenic follicles show a squamous epithelium similar to that of early previtellogenic follicles. However, this epithelium is formed by two types of cells, one similar to clear cells and the other characterized by electron dense cytoplasm filled with free ribosomes (dark cells) (Fig. 2*A*–*C*, *E*). Dark cells can have a length of over 30 μm in perpendicular section (Fig. 2*D*).

Near the apical surface in the cytoplasm, the dark cells have vesicles containing two types of particles: one about 15–25 nm and the other 25–50 nm (Fig. 2*E*). The vesicles are separated from the interface by a thin discontinuous cytoplasm. Follicle cells exhibit long processes called macrovilli that extend from the apical surface and make contact with the developing oocyte (Fig. 2*A*, *E*). Because of the development of macrovilli and vesicles, the follicle cells appear arched over the oocyte. The oocyte surface displays cytoplasmic projections called microvilli (Fig. 2*E*).

At the interface, particles identical to those of the dark cell vesicles can be observed between the macrovilli and the microvilli (Fig. 2*E*). At this stage the oocyte has endocytic invaginations that incorporate these particles, forming peripherally arranged cortical vesicles ranging from about 2 to 3 μm (Fig. 2*B*, *D*, *E*). In vitellogenic oocytes, these vesicles full of particles and membranes are present in the oocyte cortex (Fig. 3).

For examination of RNA at the ultrastructural level, thin sections of previtellogenic oocyte were incubated with the RNase–gold complex. Gold particles are present inside the cortical vesicles that contain the particulate material (Fig. 4*A*).

Pulse–chase experiments

To find out whether the follicular cells from mid-previtellogenic follicles are actively involved in the RNA synthesis, especially in the polyadenylate RNA, follicles were incubated with [^{3}H]-adenosine. In

https://doi.org/10.1017/S0967199407004297 Published online by Cambridge University Press

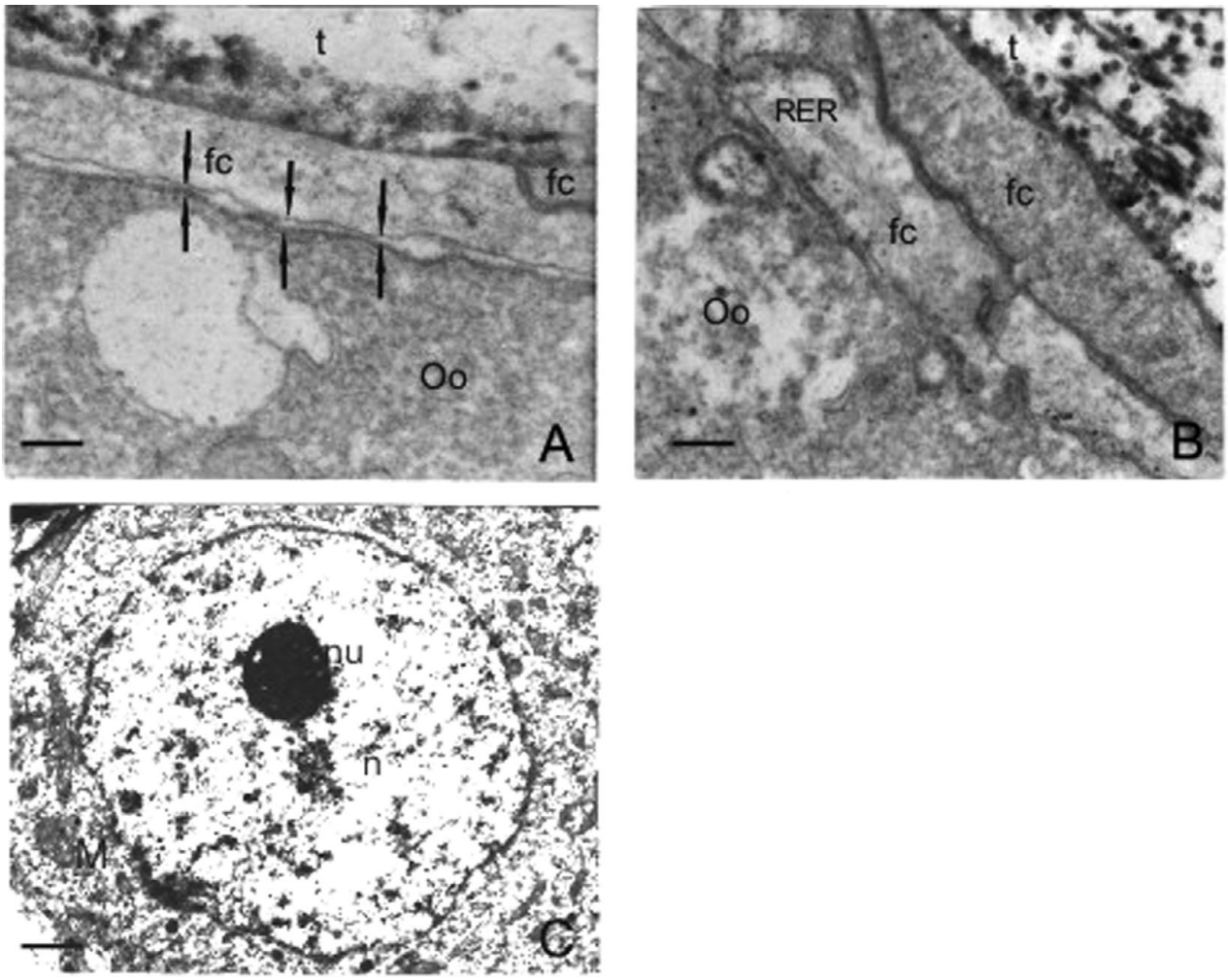

Figure 1 Electron micrographs of *C. cranwelli* early previtollogenic follicles showing the follicle cell epithelium. (*A*) Perpendicular section of the follicular epithelium. Notice that adjacent follicle cell (fc) overlap and plasma membranes of oocyte and follicle cell are in apposition (arrows). Scale bar represent 0.4 μm. (*B*) The cytoplasm is featureless, presenting few ribosomes and RER. The marginal zone shows follicle cells (fc) superposition. Scale bar represents 0.3 μm; t: theca, Oo: oocyte. (*C*) Tangential section showing the nucleus (n) and nucleolus (nu) of follicle cells; M (mitochondria). Scale bar represents 1.4 μm.

autoradiographs of a previtellogenic follicle incubated with the precursor for 5 h, intense radioactive labelling is present in the follicle cells, mainly in the nucleus and dense cluster of silver grains appear mainly in the nucleolus of the oocyte germinal vesicle Fig. 5*A*).

We carried out pulse–chase experiments to study the movement of the newly synthesized RNA. After a 5 h pulse with [^{3}H]-adenosine, previtellogenic follicles were transferred to fresh medium containing unlabelled adenosine and incubation was continued for 4 h, 9 h and 24 h. Figure 5*B–D* illustrates the distribution of the radioactive RNA after the different chase periods. As shown in Fig. 5*B*, the material labelled after 4 h of incubation was almost entirely chased into the cytoplasm of the follicle cells and after 9 h it was found between the follicle cells and the oocyte (Fig. 5C). After 24 h there was a decrease in silver deposition in the follicular cells and an accumulation of silver grains on the oocyte cortex (Fig. 5*D*).

Follicular epithelium in late previtellogenic oocytes

The monolayered epithelium in late previtellogenic follicles is formed by dark and clear cells. The dark cells partly overlap the clear cells and extend between them and the basal membrane of the epithelium (Fig. 6*A*, *B*). However, there are several regressing dark cells that present different morphological alterations characteristic of the apoptotic process. The apoptotic dark cells can be observed more clearly in a tangential than in a transverse section of the epithelium. These cells show an irregularly outlined nucleus, a large nucleolus and condensations of chromatin accumulating at the nuclear rim. The nuclear membrane in some regions is

https://doi.org/10.1017/S0967199407004297 Published online by Cambridge University Press

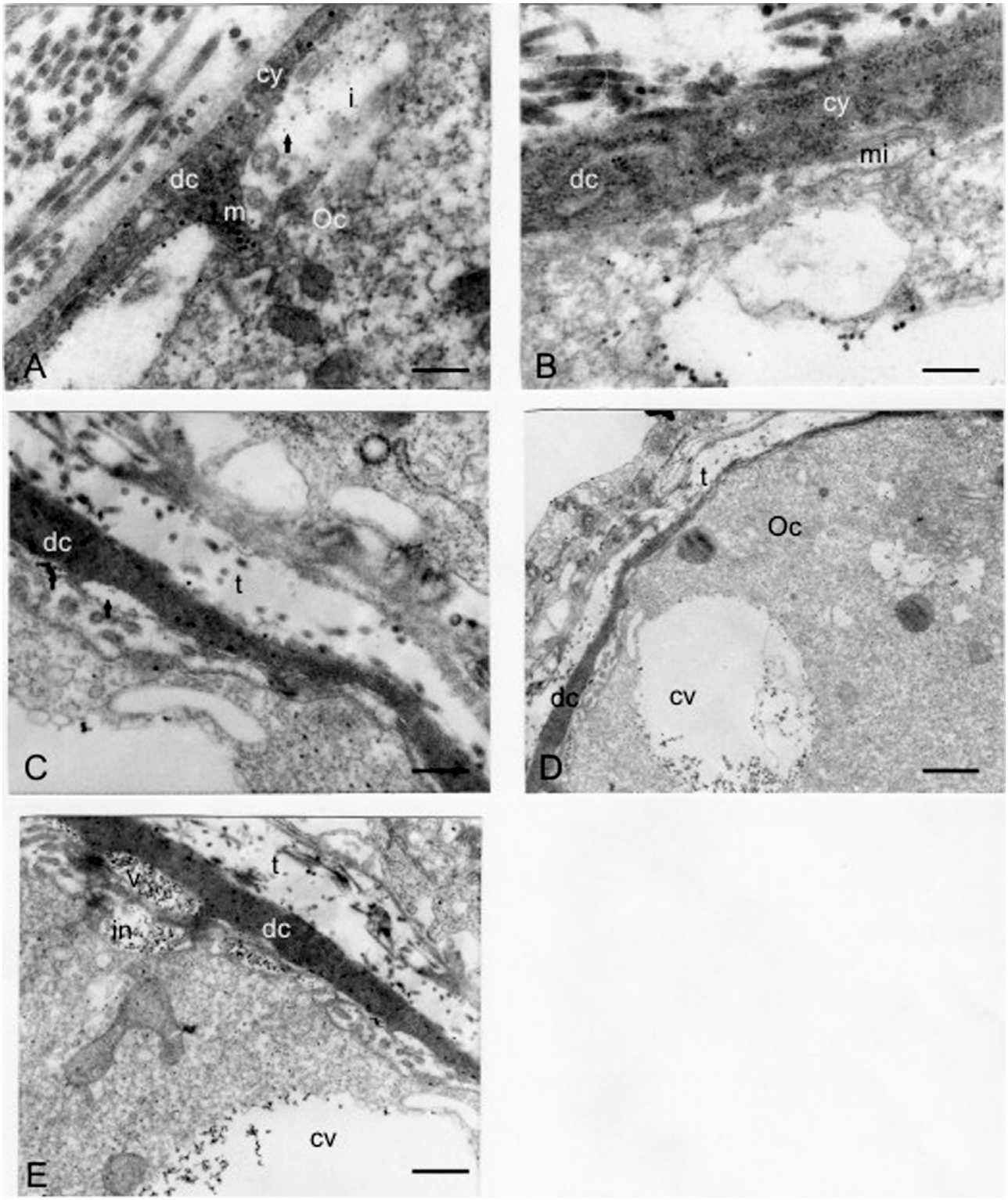

Figure 2 Electron micrograph of a *C. cranwelli* mid-previtellogenic follicle showing the follicle cell epithelium and the interface with the oocyte cortex. (*A*) Dark follicle cell (dc) with electron dense cytoplasm (cy) and a macrovilli (m) that contacts the oocyte (Oo) plasma membrane. The interface (i) shows few particles (arrow). Scale bar represents 0.3 μm. (*B*) Dark follicle cell cytoplasm (cy) with abundant free ribosomes. The interface shows a microvilli with microfilaments (mi). Scale bar represents 0.25 μm. (*C*) Dark follicle cell with vesicle in the apical surface (arrow). Scale bar represents 0.35 μm. (*D*) Long dark follicle cell (dc) surrounding the oocyte (Oo). The oocyte cortex displays cortical vesicles (cv). Scale bar represents 1.1 μm. (*E*) Dark follicle cell (dc) with a vesicle full of particles at the apical surface (v); the oocyte plasma membrane has an invagination with the same particulate material (in). The oocyte cortex also displays a cortical vesicle with the same particulate material (cv). Scale bar represents 0.7 μm; t: theca.

https://doi.org/10.1017/S0967199407004297 Published online by Cambridge University Press

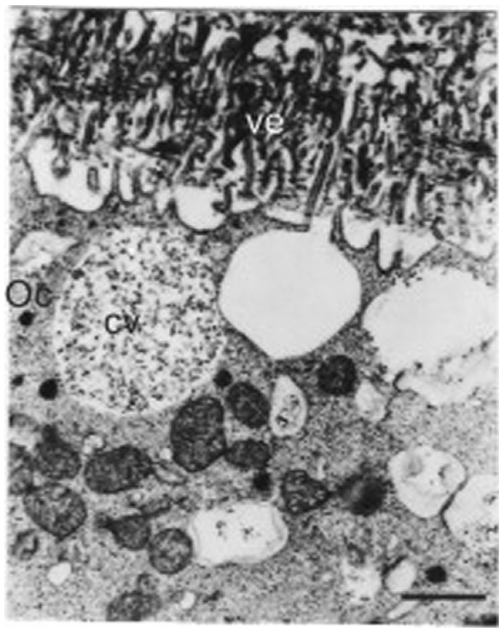

Figure 3 Electron micrograph of a *C. cranwelli* vitellogenic follicle. The oocyte (Oo) cortex shows a cortical vesicle (cv) with numerous particles; ve: vitelline envelope. Scale bar represents 1.3 μm.

swollen. The cytoplasm contains organelles but these appear less abundant than in mid-previtellogenesis (Fig. 7*A*).

Other dark cells present a more advanced stage of degeneration; there is loss of contact with adjacent cells, the cytoplasm is shrunken and the cell is surrounded by a large empty space. The nucleus presents extensive lobes with condensed chromatin and fragments of lobes near the nucleus (Fig. 7*B*). The cytoplasm of these cells contains a large number of vacuoles of various sizes, some of them with remains of chromatin or different materials and clumps of electron dense material as well as multivesicular bodies (Fig. 7*C*). Dark cell cytoplasm can also be seen between clear cells in a tangential section of the follicular epithelium (Fig. 7*D*).

On a perpendicular section in the interface, a packet of chromatin can be observed near the clear cells, which probably take up this material from the dark cells. Apoptotic bodies are clearly visible in the oocyte cortex. One or several masses of chromatin are present inside the apoptotic bodies (Fig. 6*A*, *B*).

To demonstrate nuclear DNA fragmentation, thin ovary sections were treated with the Apoptosis Detection System. Figure 8 shows no apoptotic cells in the mid-previtellogenesis stage. The first positive signal can be detected at late previtellogenesis.

Discussion

Our results demonstrate for the first time that the follicular epithelium of the amphibian *C. cranwelli* undergoes relevant modifications during the previtellogenic period of oogenesis. In the early previtellogenesis the epithelium consists of a single layer of squamous polygonal cells with clear cytoplasm. Interestingly, the boundaries of the epithelial cells are overlapping. This cytological characteristic would allow the epithelium to extend and the cells to spread over the surface of the oocyte as follicle growth goes on. The ultrastructural analysis showed that the plasma membrane of follicle cells is in close apposition to the plasma membrane of the oocyte. The interface shows no signs of an exchange of material between them.

During the mid-previtellogenic stage, two types of cells develop in the follicular epithelium: dark cells

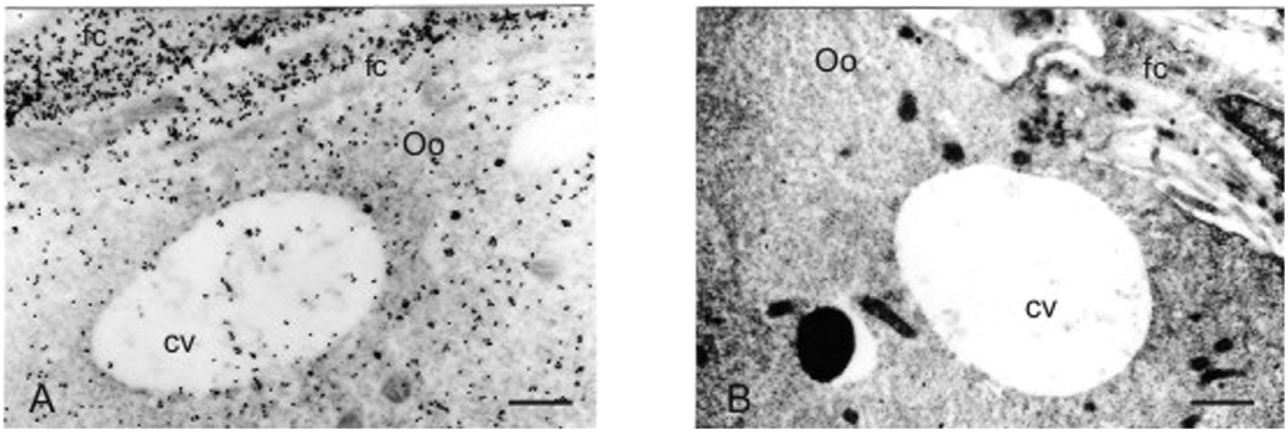

Figure 4 RNA localization by RNase–gold complex. (*A*) Electron micrograph of a mid-previtellogenic follicle incubated with RNase–gold complex showing a cortical vesicle (cv) with particles labelled inside it in the oocyte cortex. (*B*) Section of the control incubated with RNase–gold complex + RNA. No particles are present inside the cortical vesicle. Scale bar represent 0.7 μm; fc: follicle cell.

https://doi.org/10.1017/S0967199407004297 Published online by Cambridge University Press

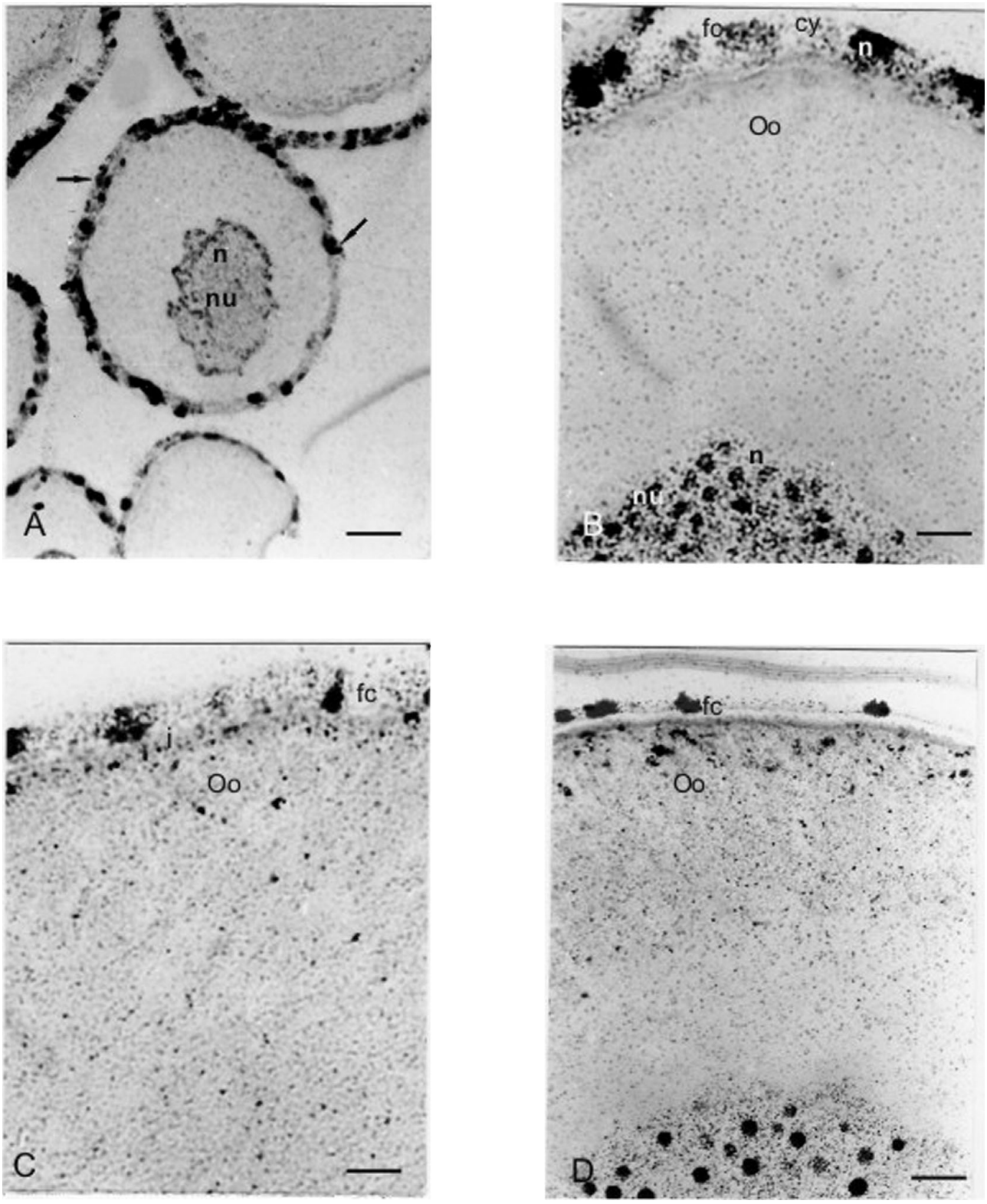

Figure 5 Pulse–chase experiments. Autoradiography sections of mid-previtellogenic follicles of *C. cranwelli* incubated for 5 h in [^{3}H]-adenosine and then transferred for 4 h; 9 h and 24 h to 1 mM adenosine solution. (*A*) Follicle section incubated for 5 h in [^{3}H]-adenosine, showing intense radioactive labelling in follicle cell nucleus (arrow) and oocyte nucleus (n) and nucleolus (nu). Scale bar represent 80 µm. (*B*) Follicle section incubated for 4 h in 1 mM adenosine solution. Radioactive labelling can be seen in the nucleus (n) and cytoplasm (cy) of the follicle cell Scale bar 20 µm. (*C*) Follicle section incubated for 9 h in 1 mM adenosine solution. The radioactive labelling can be seen in the interface between the follicular epithelium and the oocyte (i). Scale bar 20 µm. (*D*) Follicle section incubated for 24 h in 1 mM adenosine solution showing a decrease in silver deposition in the follicle cell and an accumulation of silver grain on the oocyte cortex. Scale bar represent 20 µm; fc: follicle cell.

https://doi.org/10.1017/S0967199407004297 Published online by Cambridge University Press

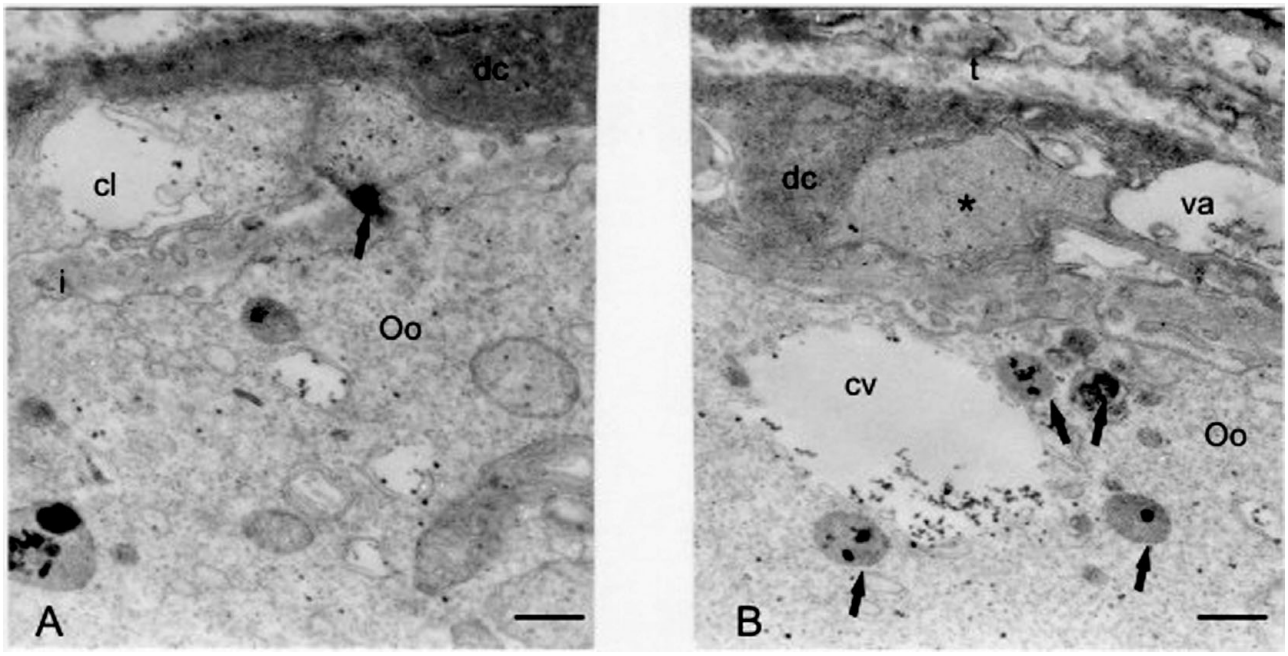

Figure 6 Electron micrograph of a *C. cranwelli* late previtellogenic follicle showing the follicular epithelium and the interface with the oocyte cortex. (*A*) The epithelium displays clear (cl) and dark cells (dc). At the periphery the dark cell body extends over the clear cell. Arrow shows chromatin near the clear cell. In the interface (i) fibrillar material, the precursor of the vitelline envelope, begins to appear. Scale bar represent 0.5 μm (*B*) Dark cell with vesicles containing fibrillar material (asterisk) and a large vacuole with smooth endoplasmic reticulum (va). The oocyte cortex has cortical vesicles (cv) and several apoptotic bodies (arrow). Scale bar represents 2 μm.

and clear cells. The dark cells appear sequentially as the stage progresses. Dark cells display ultrastructural features indicative of great synthetic activity, including large amounts of free ribosomes, glycogen, a rough endoplasmic reticulum and particle-filled vesicles. Until now, cells similar to dark cells had been described only in the avian granulosa epithelium (Callebaut, 1991).

To clarify the role of the dark cells during the growth of previtellogenic oocytes, we performed ultrastructural and autoradiographic studies. Experiments with tritiated adenosine demonstrate that the follicular cells are actively involved in RNA synthesis. Moreover, pulse–chase experiments showed the migration of the radioactive granules to the oocyte, suggesting a transfer of RNA. In the oocyte cortex, vesicles containing ribonucleoproteins appear, as shown by the RNase–gold complexes. The proposed flow of material toward the oocyte is strongly supported by the ultrastructural presence of the same vesicles with the same components in vitellogenic oocytes.

Throughout the previtellogenesis stage amphibian oocytes accumulate RNAs for their subsequent use in early embryogenesis (Davidson, 1986; Kloc *et al.*, 2002). Thus, an important characteristic of previtellogenic oocytes is the very active synthesis because of rRNA being synthesized on amplified rDNA sequences and of heterogeneous RNA being synthesized on lampbrush chromosomes. Our findings demonstrated that during mid-previtellogenesis, dark follicle cells add RNA to the oocyte cytoplasm; thus, cortical vesicles containing RNA appear in the oocyte cortex. This transfer is similar to that observed in insects and other invertebrates, where nurse cells support oocyte development by supplying nutrients, RNAs, proteins and organelles (Bonhag, 1958; King & Devine, 1958; Berry, 1985; Robinson *et al.*, 1994; Nezis *et al.*, 2003). The same process was observed in lizards between the pyriform cells and the oocyte (Andreuccetti, 1992).

The presence of cortical vesicles in *C. cranwelli* oocytes would be interpreted as an evolutionary mechanism that provides enough RNA to allow rapid oocyte development, considering that the level of RNA in the oocyte is correlated with the speed of embryonic development, as suggest by Del Pino (1989).

In this context, *C.cranwelli* previtellogenic oocytes contain high levels of RNAs not only because of gene amplification that produces multiple nucleoli, but also of the RNAs from the follicle cells present in the cortical vesicles. High RNA levels ensure a rapid development in view of the fact that this species must adapt to certain weather conditions (storms) for egg deposition to occur.

Surprisingly, as previtellogenesis progresses, a new remodelling of the follicular epithelium takes place

https://doi.org/10.1017/S0967199407004297 Published online by Cambridge University Press

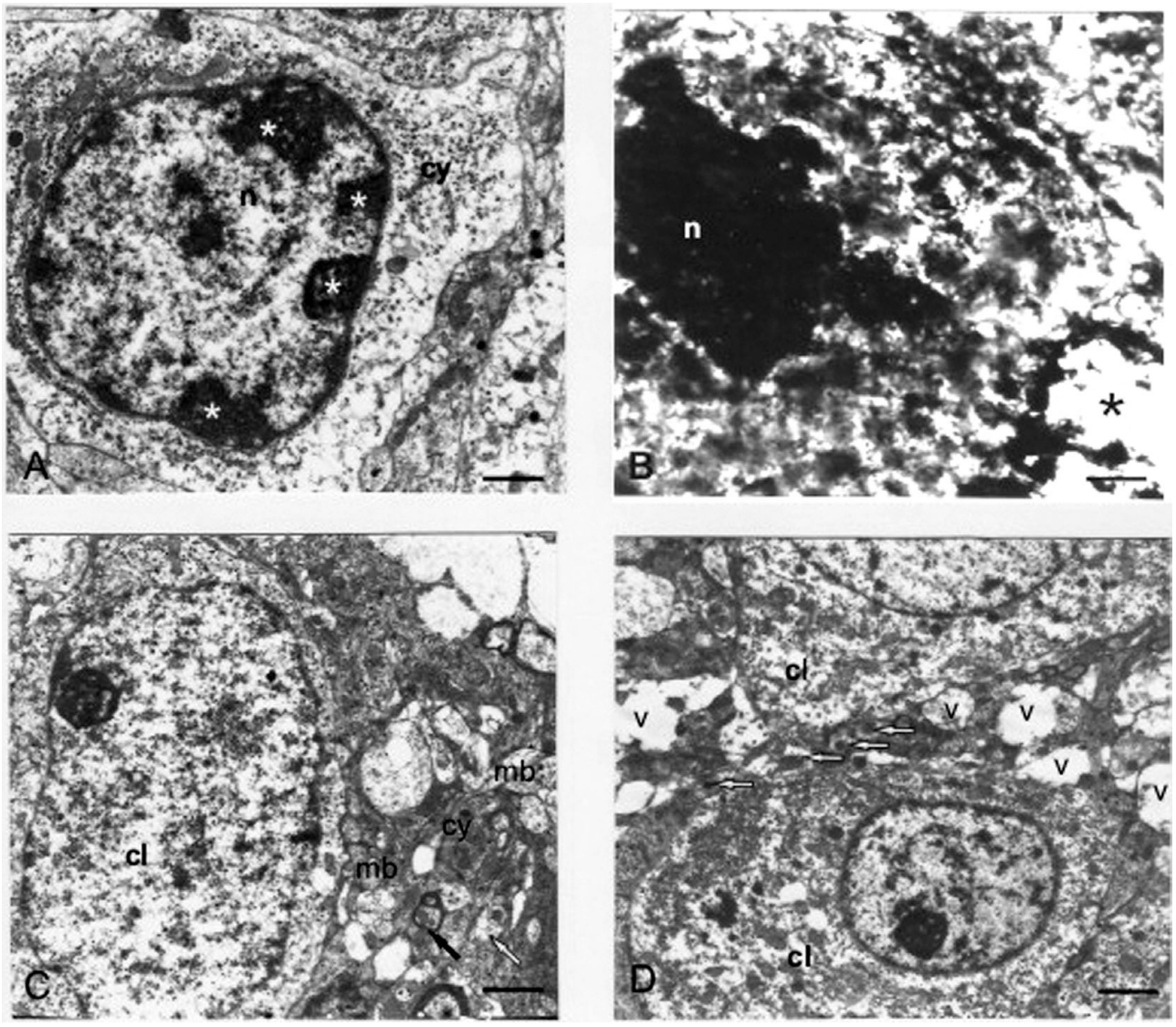

Figure 7 Electron micrograph of *C. cranwelli* late previtellogenic follicle showing tangential section of follicular epithelium. (*A*) Epithelial dark cell in early stage of regression with an irregular nucleus (n) and several patches of condensed chromatin accumulated at the nuclear membrane (asterisks). The cytoplasm (cy) contains few free ribosomes. Scale bar represents 1.4 μm. (*B*) Dark cell in late stage of degeneration showing a lobed nucleus (n) with highly condensed chromatin. Cytoplasm shrinkage produces loss of contact between adjacent cells. Note the presence of empty intercellular spaces (asterisk). Scale bar represents 1.4 μm. (*C*) Cytoplasm (cy) of apoptotic cell showing numerous vesicles, some of them with chromatin (white arrow); clumps of electron dense material (black arrow) and multivesicular bodies (mb) Scale bar represents 1.4 μm. (*D*) Two clear cells and between them the cytoplasm of dark cell with numerous apoptotic bodies (white arrows) and vesicles (v). Scale bar represents 0.5 μm.

and at the end of this stage a degeneration of dark follicle cells has evidently occurred. Our findings demonstrated that this process is associated with programmed cell death.

Degenerating cells showed the typical features of apoptosis: the condensation of chromatin around the nuclear perimeter, cell shrinkage, membrane blebbing and release of apoptotic bodies. The remodelling of the follicular epithelium was also observed in other vertebrates like the lizard *Podarcis sicula*, where the regression of the epithelium was observed by morphological and biochemical analyses (Motta *et al.*, 1996). Moreover, the same cellular mechanism was described in granulose cells in mammals (Hughes *et al.*, 1991). These findings raise the interesting possibility that programmed cell death could be a potential mechanism underlying the follicular epithelium of vertebrate oogenesis.

The apoptotic bodies released from regressing dark cells are apparently engulfed by the oocyte and can

https://doi.org/10.1017/S0967199407004297 Published online by Cambridge University Press

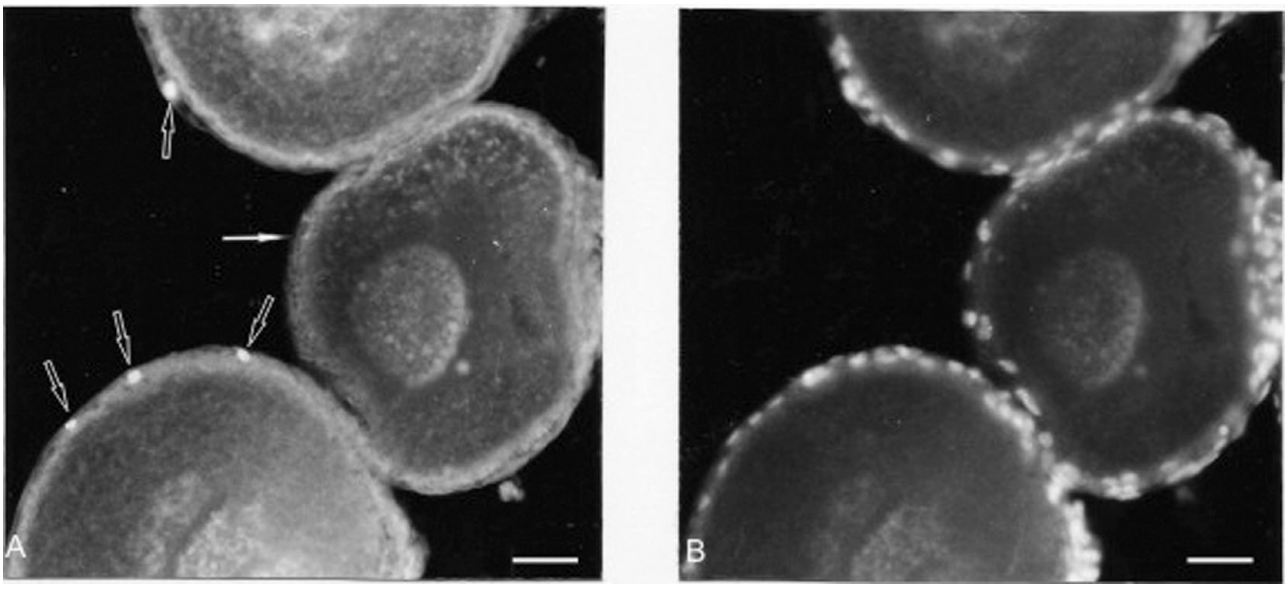

Figure 8 Light micrographs of previtellogenic oocytes double labelled with TUNEL and DAPI. (*A*) Early previtellogenic follicle; no signal of apoptosis is evident at the follicle cell epithelium (white arrow). Late previtellogenic follicle; positive signal is evident at the follicle cell epithelium (empty arrow). (*B*) The same micrograph showing the follicle cell epithelium nuclei counterstained with DAPI. Scale bar represents 30 μm.

be seen in the oocyte cortex. However, the functional significance of the apoptotic bodies inside the oocyte is unknown at present.

Our ultrastructural results evidence that during the previtellogenesis stage in the *C. cranwelli* oocyte there is a reorganization of the follicular epithelium that takes place as the oocyte grows.

Acknowledgements

This work was supported by grants to S. Sánchez from Consejo Nacional de Investigaciones Científicas y Técnicas (CONICET) and Consejo de Investigaciones de la Universidad Nacional de Tucumán (CIUNT). The authors thank Mr Enrique Dozetos for his photographic assistance and Mrs Virginia Méndez for her proofreading.

References

Ancel, P & Vitemberger, P. (1948). Recherches dur le determinisme de la symétrie bilatérale dans l'oeuf des amphibians. *Bull. Biol. Fr. Belg. Suppl.* **31**, 1–81.

Andreuccetti, P. (1992). An ultrastructural study of differentiation of pyriform cells and their contribution to oocyte growth in representative squamata. *J. Morphol.* **212**(1), 1–11.

Andreuccetti, P., Limatola, E. & Ghiara, G. (1979). Secretory activity of pyriform cells during the oocyte growth in *Lacerta sicula*. *J. Submicr. Cytol.* **11**, 369–77.

Bachvarova, R.M., Manova, K., Packer, A.I., Huang, E.J. & Besmer, P. (1992). Role of c-kit and its ligand in oocyte growth. In: *Ovarian Cell Interactions* (ed. A.J.W. Hsueh & D. Schomberg), pp. 25–37, Norwell, MA: Symposia.

Berry, S.J. (1985). RNA synthesis and storage during insect oogenesis. In: L.W. Browder (ed.): *Developmental Biology,a Comprehensive Synthesis*.New York: Plenum Press, pp. 351–84.

Bonhag, P.F. (1958). Ovarian structure and vittelogenesis in insects. *Annu. Rev. Entomol.* **3**, 137–60.

Cabada, M.O., Sánchez Riera, A.N., Genta, H.D., Genta, S.B., Sánchez, S.S. & Barisone, G.A. (1996). Vitelline envelope formation during oogenesis in *Bufo arenarum*. *Biocell* **20**, 77–86.

Callebaut, M. (1991). Pyriform-like and holding granulosa cells in the avian ovarian follicle wall. *Eur. Arch. Biol.* (Bruxelles) **102**, 135–45.

Callebaut, M. and Van, Nassauw (1987). Demonstration by monoclonal antidemin of a myoid tissue coat in the preovulatory ovarian tunica albuginea of the turtle *Pseudemys scripta elegans*. *Med. Sci. Res.* **15**, 1129–30.

Davidson, E. H. (1986). *Gene Activity in Early Development*, 3rd edn. Academic Press Inc. Orlando, Florida.

Del Pino, E.M. (1989). Marsupial frogs. *Scientific American* **260** (5), 110–8.

Dumont, J.N. (1972). Oogenesis in *Xenopus laevis* (Daudin). I. Stages of oocyte development in laboratory maintained animals. *J. Morphol.* **136**, 153–80.

Dumont, J.N. (1978). Oogenesis in *Xenopus laevis* (Daudin). VI. The route of injected tracer transport in the follicle and developing oocyte. *J. Exp. Zool.* **204**, 193–217.

Dumont, J.N. & Brummet, A.R. (1978). Oogenesis in *Xenopus laevis* (Daudin). V. Relationships between developing

oocytes and their investing follicular tissues. *J. Morphol.* **155**, 73–98.

Filosa, S. (1973). Biological and cytological aspects of the ovarian cycle in *Lacerta sicula*. *Mon. Zool. Ital.* **7**, 151–65.

Fortune, J.E. (1983). Steroid production by *Xenopus* ovarian follicles at different developmental stages. *Dev. Biol*. **99**, 502–9.

Frens, G. (1973). Controlled nucleation for the regulation of the particle size in monodisperse gold solutions. *Nature Phys. Sci.* **241**, 29.

Hernandez, A.G. & Bahr, J.M. (2003). Role of FSH and epidermal growth factor (EGF) in the initiation of steroidogenesis in granulosa cells associated with follicular selection in chicken ovaries. *Reproduction* **125**, 683–91.

Hope, J., Humphries, A.A. & Bourne, G.H. (1963). Ultrastructural studies on developing oocytes of the salamander *Triturus viridescens*. *Ultrastruct. Res.* **9**, 302–24.

Hughes, F.M. Jr, Gorospe, W.C. (1991). Biochemical identification of apoptosis (programmed cell death) in granulosa cells: evidence for a potential mechanism underlying follicular atresia. *Endocrinology* **129**(5), 2415–22.

Kemp, N.E. (1956). Electron microscopy of *Rana pipiens* oocytes. *J. Biophys. Biochem. Cytol.* **2**, 282–91.

King, R.C. & Devine, R.L. (1958). Oogenesis in adult *Drosophila melanogaster*. *Growth* **22**, 299–326.

Kloc, M., Dougherty, M.T., Bilinski, S., Chan, A.P., Brey, E., King, M.L., Patrick, C.W. Jr & Etkin, L.D. (2002). Three-dimensional ultrastructural analysis of RNA distribution within germinal granules of *Xenopus*. *Dev Biol.* **241**(1), 79–93.

Manes, M.E. & Nieto, O.L. (1983). A fast and reliable celloidin–paraffin embedding technique for yolked amphibian embryos. *Mikroskopie* **40**, 341–3.

Monroy, A., Parisi, E. & Rosati, F. (1983). On the segregation of the germ and somatic cell lines in the embryo. *Differentiation* **23**, 179–83.

Motta, C.M., Filosa, S. & Andreuccetti, P. (1995). Role of pyriform cells during the growth of oocytes in the lizard *Podarcis sicula*. *J. Exp. Zool.* **273**, 256–67.

Motta, C.M., Filosa, S. & Andreuccetti, P. (1996). Regression of the epithelium in late previtellogenic follicles of *Podarcis sicula:* a case of apoptosis. *J. Exp. Zool.* **276**, 233–41.

Motta, C.M., Tammaro, S., Cicale, A., Indolfi, P., Iodice, C., Spagnuolo, M.S. & Filosa, S. (2001). Storage in the yolk platelets of low mw DNA produced by the regressing follicle cells. *Mol. Reprod. Dev.* **59**, 422–30.

Nezis, I.P., Vassilis, M., Mpakou, V, Stravopodis, D.M., Papassideri, I.S., Mammali, I. & Margaritis, L.H. (2003). Modes of programmed cell death during *Ceratitis capitata* oogenesis. *Tissue & Cell* **35**, 113–9.

Purcell, S.M. & Keller, R. (1993). A different type of amphibian mesoderm morphogenesis in *Ceratophrys ornata*. *Development* **117**(1), 307–17.

Redshaw, M.R. (1972). The hormonal control of the amphibian ovary. *Am. Zool.* **12**, 289–306.

Robinson, D.N., Kant, K. & Cooley, L. (1994). Morphogenesis of *Drosophila* ovarian ring canals. *Development* **120**, 2015–25.

Sánchez, S.S. & Villecco, E.I. (2003). Reproductive biology and phylogeny of anura. Chapter 3, pp. 27–71. *Oogenesis* (ed.) B.J.M. Jamieson Publishers, Science Publishers, Inc., Enfield, New Hampshire, USA.

Sánchez Riera, A.N., Sánchez, S.S. and Cabada, M.O. (1988). RNA metabolism in the follicle cells of *Bufo arenarum* oocytes. *Micr. Electr. Biol. Cell.* **12**, 149–76.

Schoenfelder, M, Schams, D, Einspanier, R. (2003). Steroidogenesis during in vitro maturation of bovine cumulus oocyte complexes and possible effects of tri-butyltin on granulosa cells. *J. Steroid Biochem. Mol. Biol.* **84**, 291–300.

Sretarugsa, P. & Wallace, R.A. (1997). The developing *Xenopus* oocyte specifies the type of gonadotropin-stimulated steroidogenesis performed by its associated follicle cells. *Dev. Growth Differ*. **39**, 87–97.

Tinsley, R.C., Loumont, C. & Kobel, H.R. (1996). Geographical distribution and ecology. In: *The Biology of Xenopus*. R.C. Tinsley & H.R. Kobel (eds). Oxford. Oxford University Press, pp. 35–39.

Villecco, E.I. (1998). Ovogénesis en anfibios: interacciones celulares. Doctoral dissertation, Universidad Nacional de Tucumán, Tucumán, Argentina.

Villecco, E.I., Aybar, M.J., Sanchez, S.S. & Sanchez Riera, A.N. (1996). Heterologous gap junctions between oocyte and follicle cells in *Bufo arenarum:* hormonal effects on their permeability and potential role in meiotic arrest. *J. Exp. Zool.* **276**, 76–85.

Villecco, E.I., Aybar, M.J., Genta, S.B., Sánchez, S.S. & Sánchez Riera, A.N. (2000). Effect of gap junction uncoupling in full-grown *Bufo arenarum* ovarian follicles: participation of cAMP in meiotic arrest. *Zygote* **8**, 171–9.

Wartenberg, S. & Gusek, W. (1960). Electron microscopic research on the fine structure of the ovarian ovum and the follicular epithelium of amphibia. *Expt. Cell. Res.* **19**, 199.